Ceramics-Silikáty 65 (2), 132-140 (2021)
www.ceramics-silikaty.cz doi: 10.13168/cs.2021.0012

THE EFFECT OF NANO-$CaCO_3$ ON THE PROPERTIES OF BMSC

JIANG XINGHAN*, ZHOU JIAQI*, #WU CHENGYOU*, **, KOU XIHU*, LIU PANPAN*

*School of Civil Engineering, Qinghai University, Xining 810016, PR China
**Key Laboratory of Building Energy-saving Materials and Engineering Safety of Qinghai Province, Xining 810016, PR China

#E-mail: wuchengyou86@163.com

Submitted January 25, 2021; accepted February 22, 2021

Keywords: Nanomaterial, Compressive strength, Microstructure, Hydration heat release, Water resistance

In this work, to study the effects of different contents of nano-$CaCO_3$ on the hydration characteristics of a basic magnesium sulfate cement (BMSC), the mechanical properties and water resistance of the BMSC paste were analysed via compressive strength tests and long-term immersion tests. The effect of nano-$CaCO_3$ on the hydration of the BMSC was studied via X-ray diffraction, scanning electron microscopy, and a hydration exothermic curve analysis. The results showed that the early strength and water resistance of the BMSC paste can be improved by different dosages of nano-$CaCO_3$, and the optimum dosage was found to be 3 %. Moreover, the addition of nano-$CaCO_3$ will not affect the setting and hardening time of the BMSC, nor will it change the phase composition and micromorphology of the BMSC.

INTRODUCTION

Basic magnesium sulfate cement (BMSC) is a MgO–$MgSO_4$–H_2O ternary cementitious material, which is prepared by mixing an active MgO (α-MgO) powder, a $MgSO_4$ solution of a certain concentration, and an appropriate additive (e.g., sodium citrate) in a certain proportion [1-2]. The main hydration product is a dense structure of insoluble basic magnesium sulfate whiskers ($5Mg(OH)_2 \cdot MgSO_4 \cdot 7H_2O$), which are characterised as having low density, high early strength, high strength, high-temperature resistance, corrosion resistance, and carbonisation resistance [3-7]. Compared with common Portland cement, BMSC has many advantages, such as good toughness (the flexural strength is twice that of normal Portland cement under the same compressive strength), but the setting time of BMSC pastes is slow [5].

Nanotechnology has a wide range of applications, and nanomaterials have a small size effect, surface effect, volume effect, and macro-quantum tunnelling effect [8-9]. Therefore, they exhibit many unique properties and are widely used in catalysis, light-filtering, light absorption, medicine, magnetic media, and new materials [10-12]. In recent years, nanomaterials have gradually become a research hotspot in the field of building materials [13-16]. One of the most common applications is the incorporation of nanomaterials into cement pastes. By filling the pores between the cement particles with nanomaterials, the porosity of the cement paste can be reduced, and the compactness of the cement paste can be improved; therefore, the mechanical properties of the cement paste can be remarkably enhanced [17-18].

The effects of various nanomaterials on the mechanical properties and microstructures of cement pastes have previously been studied. For example, Rajeev Roychand et al. [19] studied the effect of nano-SiO_2 on the physical and chemical properties of cement pastes with high contents of fly ash. Feng et al. [20] studied the dispersion of nano-SiO_2 in the early hydration of cement pastes. Nazari et al. [21] studied the effect of nano-ZnO on the flexural strength of self-compacting concrete. To improve the microstructure of self-compacting mortar and reduce the microvoidage, Ahmed [22] added nano-cement kiln ash into the self-compacting mortar; the results revealed that the compressive strength, direct tensile strength, and flexural strength of the self-compacting mortar increased with an increase in the nano-powder content. However, the preparation of these nanomaterials is difficult, which limits their large-scale use. Thus, nanomaterials are rarely mixed with cement paste in construction project applications.

The calcium carbonate ($CaCO_3$) content in nature is relatively abundant, and the replacement of expensive nanomaterials with $CaCO_3$ is both economical and reasonable. Wang et al. [23] studied the effect of nano-$CaCO_3$ on the hydration properties of cement, and found that the addition of nano-$CaCO_3$ can increase the hydration heat

release rate and total heat release of a cement, thereby improving its early strength. Tao et al. [24] studied the effect of nano-$CaCO_3$ pastes on the mechanical properties and microstructures of a cement concrete, and found that, after adding nano-$CaCO_3$ pastes into the concrete, the filling effect of nano-$CaCO_3$ accelerated the hydration process of the cement and increased the early compressive strength of the concrete. Additionally, the effect of nano-$CaCO_3$ on the pore structure of carbon fibre-reinforced concrete (CFRC) was studied by Liu et al. [25], who found that the addition of nano-$CaCO_3$ can prevent the occurrence of overlapping defects by preventing overlapping fibres. Moreover, the porosity of the microstructure of the CFRP-reinforced concrete was low, the interconnectivity of the micropores was avoided, and the permeability of the concrete was remarkably improved.

Existing research on the influence of nano-$CaCO_3$ on the performance of cement concrete has primarily been focused on Portland cement; in contrast, little research on the modification of BMSCs with nano-$CaCO_3$ exists. Thus, the effects of nano-$CaCO_3$ on the BMSC properties were investigated in this research. The BMSC properties of were tested by X-ray diffraction (XRD) and scanning electron microscopy (SEM), and the mechanism of the modification of the BMSC by the nano-$CaCO_3$ is further explained from the perspectives of the cement microstructure and phase composition of the hydration products.

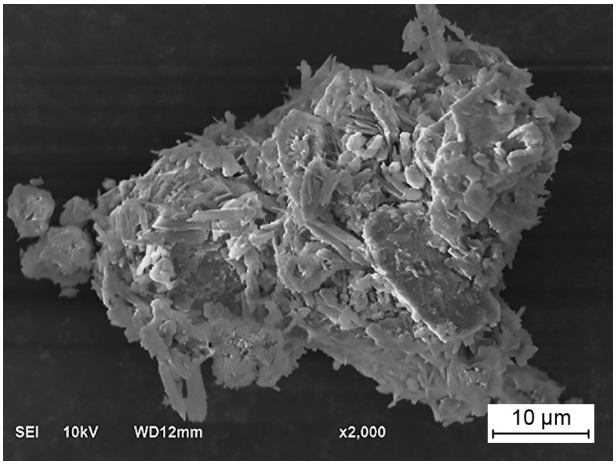

Figure 1. Electron micrograph of the nano-$CaCO_3$ (2000×).

EXPERIMENTAL

Raw materials

Magnesia powder is a light-burned powder made by calcining magnesite (in this study, the magnesite was sourced from Dashiqiao, Liaoning Province) at 750-850 °C and then grinding it. The content of the active MgO used in this study was 59.04 %, as determined by the hydration method and its chemical composition and content are reported in Table 1.

Table 1. Chemical composition of the burnt magnesia powder.

Composition	MgO	CaO	SiO_2	Al_2O_3	Fe_2O_3	CO_2
Content (%)	80.20	1.30	6.07	0.15	0.41	11.87

Table 2. Basic parameters of the nano-$CaCO_3$.

Nano-$CaCO_3$	
Colour	white
Shape	powdered form
Particle size	40 nm
Purity	≥ 99.9 %
Impurity	≤ 0.1 %

The magnesium sulfate solution was composed of $MgSO_4 \cdot MgS_2O$ crystals (purchased from Tianjin Comeo Chemical Co., Ltd.) and deionised water with a molar ratio of 1:13, i.e., the molar ratio of $MgSO_4$ to H_2O was 1:20.

The sodium citrate used in this study was manufactured by Tianjin Zhiyuan Chemical Reagent Co., Ltd. The purity was not less than 99 %, and the pH (50 $g \cdot l^{-1}$) was 7.5 - 9.0. The nano-$CaCO_3$ used in this study was produced by Beijing Boyu Hi-tech New Material Technology Co., Ltd. The purity was not less than 99.9 %, and the average particle size was not more than 40 nm.

Preparation, maintenance, and testing of the specimens

Preparation and maintenance of the specimens

To prepare the BMSC, the molar ratio of the activated MgO to magnesium sulfate (α-MgO/$MgSO_4$) was first calculated.

Then, the appropriate amount of the MgO powder was weighed, and the mass of the $MgSO_4$ solution (1:20) was calculated according to the molar ratio. The mass of the MgO was 0.5 % of the mass of the sodium citrate. The nano-$CaCO_3$ was mixed with the raw material powder particles, after which the $MgSO_4$ solution was added and stirred for 50 s to form a uniform BMSC slurry. The mix proportion design is reported in Table 3.

Finally, the BMSC paste was rapidly injected into a steel mould of 20 × 20 × 20 mm^3 in size, which was coated with mineral oil or a mould release agent and fully vibrated. Any excess paste on the surface was then scraped off with a scraper, and the surface was covered with a protective film to prevent water evaporation. The mould was then removed after curing at 20 ± 5 °C and 35 ± 15 % humidity for 1 d. The experiments were carried out after 3, 7, and 28 d of natural curing at room temperature.

Table 3. Mix proportion design.

Specimen label	Molar ratio (α-MgO/$MgSO_4$)	NCa content (mass ratio: NCa/MgO)	Ca content (mass ratio: Ca/MgO)	Water-cement ratio (W/C)
C	8	0	0.5%	0.54
NCa1	8	1%	0.5%	0.54
NCa2	8	2%	0.5%	0.54
NCa3	8	3%	0.5%	0.54
NCa4	8	4%	0.5%	0.54
NCa5	8	5%	0.5%	0.54

Note: C represents the blank control, and NCa represents nano-$CaCO_3$; the different numbers (1, 2, 3, 4, 5) represent the different test groups with different contents of nano-$CaCO_3$. For example, NCa1 represents the first set of experiments; the molar ratio of the active MgO to $MgSO_4$ was 8, the content of the nano-$CaCO_3$ was 1% (the mass ratio of the nano-$CaCO_3$ to MgO), the sodium citrate content was 0.5% (the mass ratio of the sodium citrate to MgO), and the water-cement ratio was 0.54 (the mass ratio of the water to MgO and $MgSO_4$).

Performance test of the specimens

According to the GB 175-2007 specification, the compressive strength of a cement slurry should be tested by a testing machine at a constant loading speed of 0.3 kN/s. In this research, the compressive strengths of the cement pastes with different ratios of nano-$CaCO_3$ were measured on days 1, 3, 7, and 28, and the effect of nano-$CaCO_3$ on the strength of the BMSC pastes was analysed.

The water resistance of the cement paste test specimen, i.e., its ability to resist water erosion, is reflected by the softening coefficient, which is the ratio of the strength of the 28-day-old specimen to that of the 28-day-old specimen after immersing it in water for 30 days, and it was used as an index to judge the water resistance of the specimen.

The types and microstructures of the hydration products were analysed by XRD and SEM to determine the mechanism of the change of the strength of the cement paste. The BMSC was ground into a powder (D90 < 35 μm), and the crystal phase composition of the hydrated product of the cement was detected when the acceleration voltage of the X-ray diffractometer (D/max-2500PC) was 30 kV and the scanning area (2θ) was 5 - 70 °C. HighScore software was used to determine the types of crystalline phases. The microstructures of the magnesium oxysulfate samples were observed by a scanning electron microscope (JSM-5610V).

According to the GB/T 12959-2008 standard, a Calmetrix-I-Cal 4000HPC four-channel isothermal calorimeter was used to test the heat release rate of the BMSC hydration with different mixture ratios.

RESULTS AND DISCUSSION

Strength analysis

Figure 2 presents the strengths of the BMSC pastes mixed with different amounts of nano-$CaCO_3$ measured on days 1, 3, 7, and 28. The strength of the cement paste was found to increase with the curing time, and the rate of strength increase decreased with time. This is because, with the increase of the curing time, the hydration process of the cement is more complete, more hydration products are produced, and the strength of the cement paste increases; the constant consumption of the reactants results in a decrease in the concentration, which slows down the hydration rate and the increase in strength.

In addition, the compressive strength of control group C without the addition of nano-$CaCO_3$ was lower than those of the experimental group at different ages, which demonstrates that the addition of nano-$CaCO_3$ could improve the early compressive strength of the BMSC; however, the effect of the nano-$CaCO_3$ on the compressive strength was small. The 1 day compressive strength of the control group was 14.5 MPa, and that of the experimental group was 18.9 MPa, exhibiting an improvement of 30.3 %. With an increase in the curing time, the increasing trend of the compressive strength of the experimental group was gradually weakened. On day 28, the compressive strength of the control group was 74.2 MPa, and that of the experimental group was 85.4 MPa, exhibiting an improvement of 15.1 %. From these data, it is evident that nano-$CaCO_3$ can improve the early strength of cement pastes, but not the late strength. The reason for this phenomenon may be that, after the addition of nano-$CaCO_3$, the early hydration

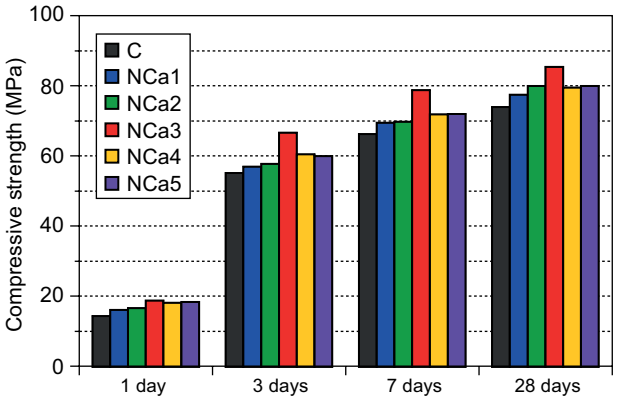

Figure 2. Effects of the different nano-$CaCO_3$ contents on the compressive strength of the BMSC paste.

process of the cement is promoted by the nucleation of nanomaterials and more hydration products are produced, thereby greatly increasing the early strength of the cement.

With an increase in the curing time, the ion concentration of NCa3 was less than that in the control group at a later stage of cement hydration, the rate of hydration was lower than that of the control group, and the strength phase of the control group was also lower; thus, the strength increase of the control group was higher than that of the experimental group.

As can be seen from Figure 2, from day 7 to 28, the compressive strengths of NCa3 and the control group increased by 5.3 MPa and 4.0 MPa, respectively. The higher compressive strength of NCa3 as compared to that of the control group may be due to the smaller size of nano-$CaCO_3$, which exerted a filling effect on the cement paste, thereby optimising the pore structure and increasing the strength of the paste.

From the development trend of the compressive strength of NCa3, it can be seen that the mechanical properties of NCa3 were good, and the compressive strength of NCa3 increased with an increase in the nano-$CaCO_3$ content; when the content reached 3 %, the compressive strength of the specimen reached its peak and then exhibited a decreasing trend. In consideration of the results of previous research on silicon dioxide, a possible reason for this phenomenon is that the particle size of the nano-$CaCO_3$ is smaller than that of the cement particles. With an increase in the nano-$CaCO_3$ content, the pore structure inside the paste was optimised due to the filling effect of the nano-$CaCO_3$, and the strength of the BMSC was improved; however, with an increase in the cement content, the excess nano-$CaCO_3$ could not fill the pores, thereby leading to a slight decrease in strength.

XRD and SEM analysis

To study the effect of the nano-$CaCO_3$ on the early compressive strength of the BMSC, it was necessary to conduct XRD tracing experiments on the specimens, and a further analysis was conducted to determine the composition of each crystal phase of the cement.

Figure 3 presents the phase composition of the BMSC with the different nano-$CaCO_3$ contents after curing for 1 d. The main hydration products in the cement paste were 517-phase MgO and $Mg(OH)_2$. The results indicate that the addition of nano-$CaCO_3$ did not change the phase composition of the cement hydration products.

Additionally, the intensity of the MgO diffraction peak in the control group was higher than that in the experimental group with the different nano-$CaCO_3$ contents, and the intensity of the diffraction peak of the produced 517 phase was lower than that in the experimental group; the 517 phase was the main strength phase of the BMSC. The results indicate that the addition of nano-$CaCO_3$ can accelerate the hydration process of the BMSC. The possible reason for this result is that the specific surface area of the nano-$CaCO_3$ is very large, as is its contact area with other reactants; thus, the hydration reaction of the cement was accelerated. Moreover, the volcanic ash effect of the nano-$CaCO_3$ can also promote the hydration process of the cement.

In the BMSC specimens with the different nano-$CaCO_3$ contents, the content of the 517 phase was the highest in NCa3, while the content of magnesia was the least, which demonstrates that a 3% nano-$CaCO_3$ content can better promote the formation of the 517 phase; increasing the strength of the BMSC and increasing the amount of 517 phases are the fundamental reasons for the increase in the early compressive strength of the cement.

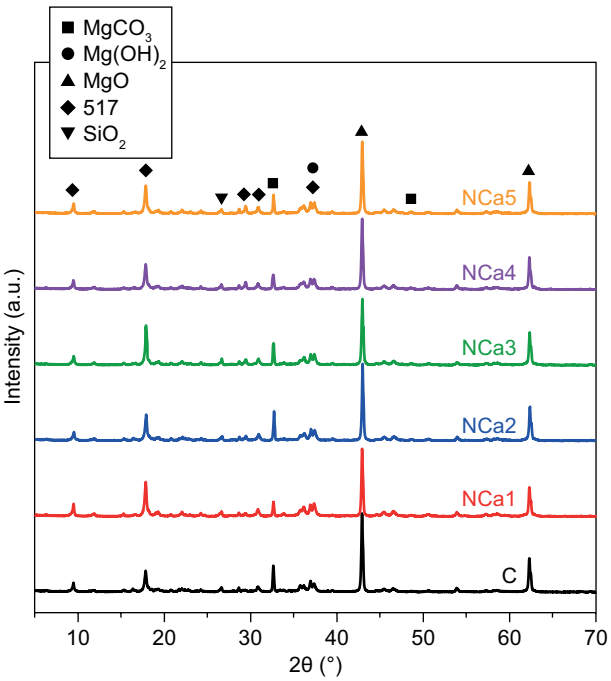

Figure 3. XRD results of the BMSC with the different nano-$CaCO_3$ contents.

The microstructures of the hydrated products of the BMSC with the different nano-$CaCO_3$ contents were analysed by SEM. Figure 4 displays the SEM images of the BMSC with the different contents of nano-$CaCO_3$ after curing for 1 d.

Group NCa3 and the control group were selected as the research objects. The results showed that the main strengthening 517 phase of the hydration products of the two groups had needle-like crystal structures, and the addition of nano-$CaCO_3$ did not change the micromorphology of the 517 phase, however, there were subtle differences. As shown in Figure 4a, the 517 phase of the control group was spread out from the centre and was partially lumpy, and the $Mg(OH)_2$ was embedded in the pores. As shown in Figure 4b, the 517 phase of

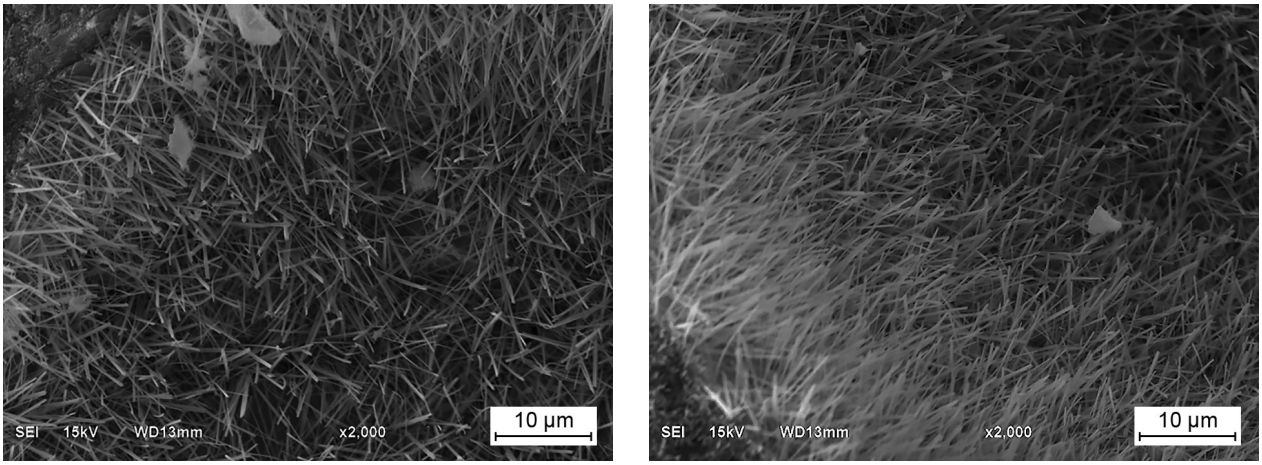

a) Control group b) NCa3 group

Figure 4. SEM images of the BMSC with the different nano-$CaCO_3$ contents after curing for 1 d (2000×).

group NCa3 was relatively denser and the number of massive $Mg(OH)_2$ particles between the pores was less than that in the control group, which provides support for the strength of the BMSC. Ultimately, the change in the hydration space structure was found to be one of the reasons for the change in strength.

Effect of the different contents of nano-$CaCO_3$ on the water resistance of the BMSC

To study the effect of the different contents of the nano-$CaCO_3$ on the water resistance of the BMSC, the compressive strengths of the soaked cement specimens were tested. The softening coefficient is used to describe the water resistance, and the data were fitted with the Origin software. The softening coefficient is a parameter of water resistance, and is expressed by the softening coefficient of the material, the unconfined compressive strength of the material under water saturation conditions (MPa), and the unconfined compressive strength of the material under dry conditions (MPa).

Figure 5 presents the compressive strength and softening coefficient of the BMSC specimens after immersion in water. The compressive strength and softening coefficient of the experimental and control groups exhibited decreasing trends after immersion in water, and those of the control group were lower than those of the experimental group after immersion in water for different amounts of time. Moreover, the decrease in the compressive strength in the control group was much larger than that in the experimental group.

After immersion in water for 60 d, the surface of the test specimen in the control group was found to be cracked, and its surface even exhibited some surface flaking. Compared with the control group, the experimental group including specimens with different nano-$CaCO_3$ contents still had a higher compressive strength and smoother surface after 60 d of immersion. Among them, group NCa3 had the best water resistance. After

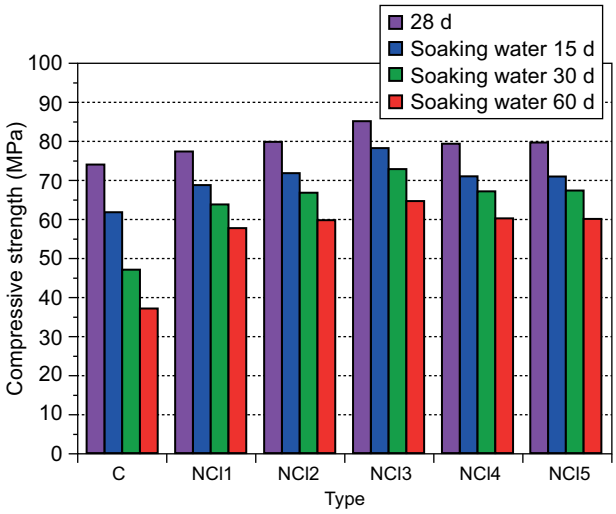

a)

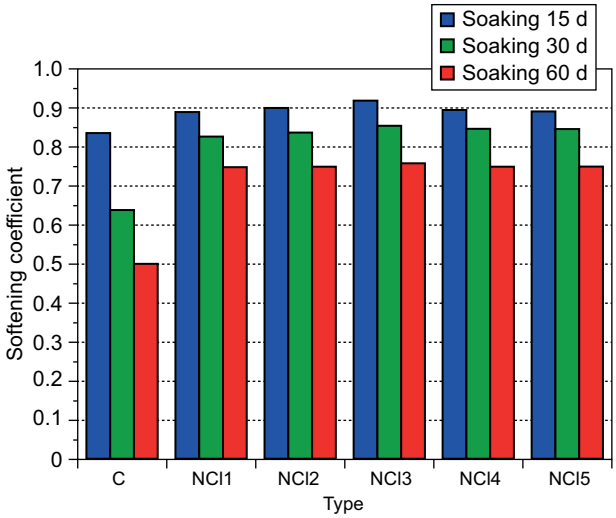

b)

Figure 5. Compressive strength and water resistance of the BMSC with the added nano-$CaCO_3$ after soaking.

60 d of immersion in water, the compressive strength and softening coefficient of the control group were 37.2 MPa and 0.50, respectively, and those of the experimental group were 64.8 MPa and 0.76, respectively, exhibiting respective increases of 74.19 % and 52 %. The results indicate that the addition of 3 % nano-$CaCO_3$ can improve the water resistance of the BMSC.

To further explore the mechanism by which the nano-$CaCO_3$ improves the water resistance of the BMSC, the specimens in the control group and the experimental group NCa3 before and after immersion were selected for the XRD investigation of the phase compositions of the hydration products. As the experimental group NCa3 exhibited good mechanical properties, it was taken as the main research object. Figure 6 presents the XRD patterns of the BMSC before and after immersion, from which it is evident that the phase composition of the main hydration phase of the BMSC was unchanged after soaking; the 517 phase and MgO remained, as did the SiO_2 and $MgCO_3$ from the raw materials. After immersing the BMSC in water for 60 d, the intensity of the MgO diffraction peak decreased substantially, the intensity of the $Mg(OH)_2$ diffraction peak increased further, and a small amount of the 517 phase was enhanced.

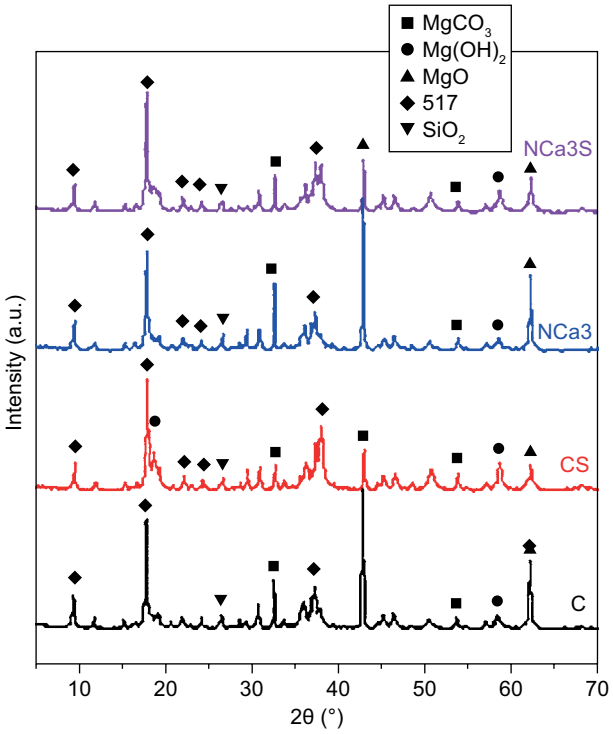

Figure 6. XRD patterns of the BMSC before and after soaking.

The reason for this phenomenon may be that a small amount of low-activity MgO in the raw material had been slowly hydrated in the long-term water environment, resulting in the weak alkalinity of the water environment; simultaneously, the MgO reacted with the unreacted hydrated $MgSO_4$ to form a small amount of 517-phase crystals. However, the main reason for the decrease in the strength of the BMSC is due to the secondary hydration of most of the remaining MgO in the water, which led to the formation of lamellar $Mg(OH)_2$ with a lower density in the cement paste. As a result, the slurry structure gradually became loose and cracks ultimately appeared, which reduced the strength of the test specimen. It can also be seen from Figure 6 that the intensity of the diffraction peak of $Mg(OH)_2$ in the experimental group after immersion in water was further reduced when compared with that in the control group; thus, the hydration of the BMSC in the water was inhibited to form the crystallisation phase of $Mg(OH)_2$, which is disadvantageous to the strength of the cement. However, it protected the crystals and effectively prevented the massive hydrolysis of the 517 phase; therefore, the high strength of the BMSC was maintained, and its water resistance was improved.

The micromorphologies of the hydration products of the BMSC before and after soaking were analysed

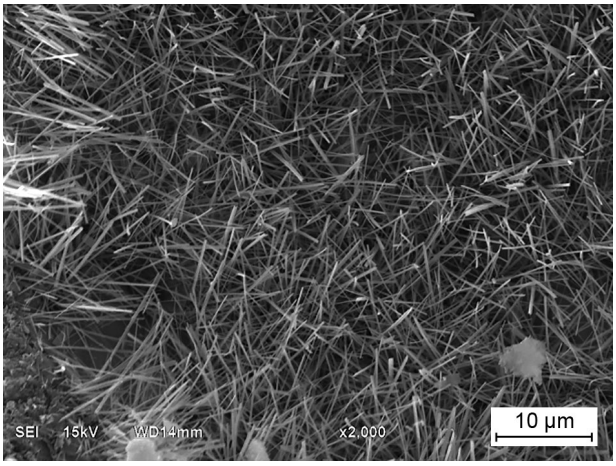

a) C-28d (2,000×)

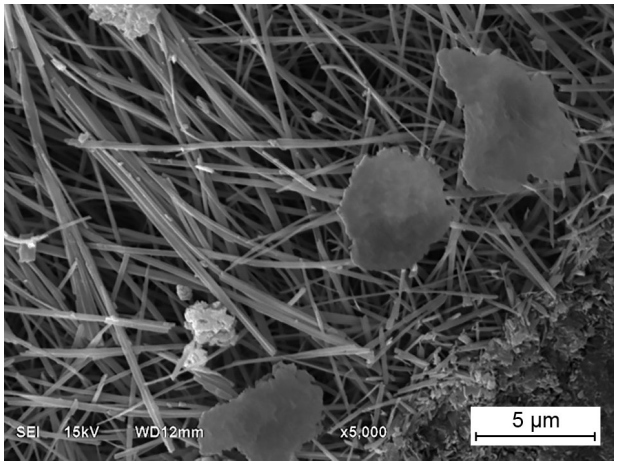

b) CS (5,000×)

Figure 7. SEM images of the BMSC before and after soaking. *(Continue on next page)*

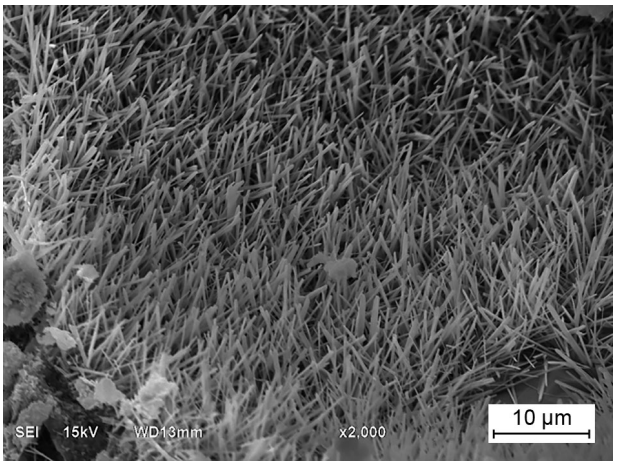

c) NCa3-28d (2,000×)

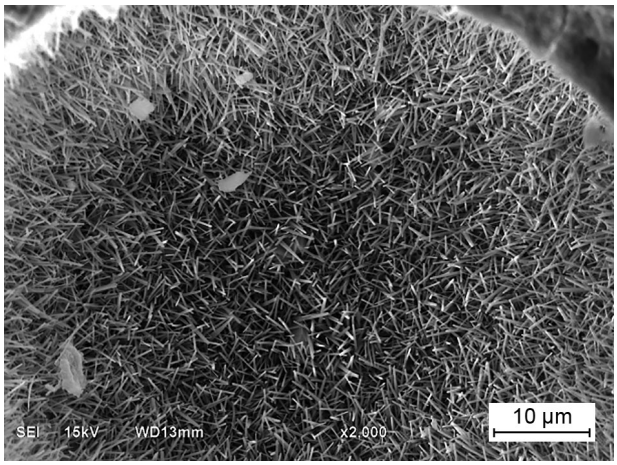

d) NCa3S (2,000×)

Figure 7. SEM images of the BMSC before and after soaking.

by SEM. As presented in Figures 7a and b, there were many needle-like materials in the BMSC before it was immersed in the water. Many acicular materials were the main hydrate crystals of the BMSC slurry, i.e., the 517 phase. After soaking in water, the needle-like materials in the pores obviously changed; they became thin and entwined with each other, and a portion of the 517 phase was hydrolysed to form a massive and flaky $Mg(OH)_2$ crystal phase, the strength of which was much lower than that of the 517 phase. In addition, the high porosity and loose structure of the slurry caused the water to contact the inner crystals, which caused the crystals to continuously hydrate and led to poor water resistance. As shown in Figures 7c and d, a large number of needle-tip-like 517-phase crystals were observed in the BMSC with the added nano-$CaCO_3$ before and after the water immersion. The only difference is that the whiskers of the NCa3 sample were shorter than those of the 517 phase before soaking, and the crystal shape changed from needle-like to rod-like, which provided strength support for the BMSC. Moreover, the main 517 hydration phase remained interlaced after soaking, and the further hydrolysis of the 517-phase crystals was avoided, which ultimately improved the water resistance of the BMSC.

Hydration heat of the BMSC with the different nano-$CaCO_3$ contents

Figure 8 presents the hydration exothermic curves of the BMSC with the different nano-$CaCO_3$ contents. With an increase in the nano-$CaCO_3$ content, there was no obvious change in the time nodes of the five stages of the hydration process of the BMSC. This indicates that the addition of nano-$CaCO_3$ did not affect the setting and hardening time of the cement, and also exerted no retarding or accelerating effect.

In the initial stage of cement hydration, the hydration rate was faster, but then rapidly reduced and maintained a lower value for a period of time. This is because, at the beginning of the cement hydration, the specific surface area of the cement particles was larger, as was the contact area with reactants, which led to a faster hydration rate. Moreover, during the reaction, a hydration film was formed on the surface of the cement particles, which encased them and prevented a cement reaction, ultimately leading to a reduction in the hydration rate in the early stage.

The hydration rate was maintained at a low level because the cement particles were surrounded by a layer of hydration film, and the reactants could not sufficiently touch them. The pH value of the solution increased with the hydration reaction. When the pH value reached a certain value, the hydration film on the surface of the cement particles was gradually destroyed, increasingly more cement particles made contact with the solution again, the hydration rate began to gradually increase, and the hydration process of the cement entered an accelerating period. When the hydration film on the surface of the cement was completely destroyed, the cement particles were in full contact with the solution, and the hydration rate of the cement reached the maximum. With further hydration, the specific surface area and surface energy of the cement particles both decreased again, at which time the hydration rate of the cement began to slow down and the hydration process entered the deceleration period. With the further development of the cement hydration, the amounts of the solution and cement gradually decreased. When certain values were reached, the cement hydration rate remained at a lower level and exhibited a slowly declining trend; at this time, the cement hydration process entered a stable period.

As can be seen from Figure 8b, the maximum exothermic rate of the BMSC with the different contents of nano-$CaCO_3$ occurred between 14.4 and 16.5 h per unit time. The maximum cement hydration rate of NCa3 was the lowest and occurred at the latest time. As presented in Figure 8c, the experimental group had the highest total amount of nano-$CaCO_3$. The maximum heat release rate

of NCa3 was the minimum of all the test groups, which demonstrates that the temperature stress produced in the process of the cement setting and hardening was the minimum. Moreover, the total heat released during the cement hydration of NCa3 was the maximum of all the test groups; therefore, the compressive strength of NCa3 was the best, which is in agreement with the previous measurements.

The maximum exothermic rate of the experimental group was lower than that of the control group, which may be due to the decrease in the reaction amount of the cement particles. As shown in Figure 8c, in addition to experimental group NCa5, the hydration heat release rate of the BMSC was reduced, which is of great significance in preventing the cracking of concrete in practical engineering applications. Additionally, compared with the control group, the other experimental groups had higher total amounts of hydration heat, among which, that of the BMSC with a 3 % content of nano-$CaCO_3$ was the best. The more heat released in the early stage, the more hydration products formed in the hydration process, and the more obvious the increase of the 517 phase was. Additionally, because the 517 phase is the strength phase, the effect of the early strength increase of group NCa3 was obvious. This also proves that the increase of the 517 phase is the main reason for the early strength increase of the cement.

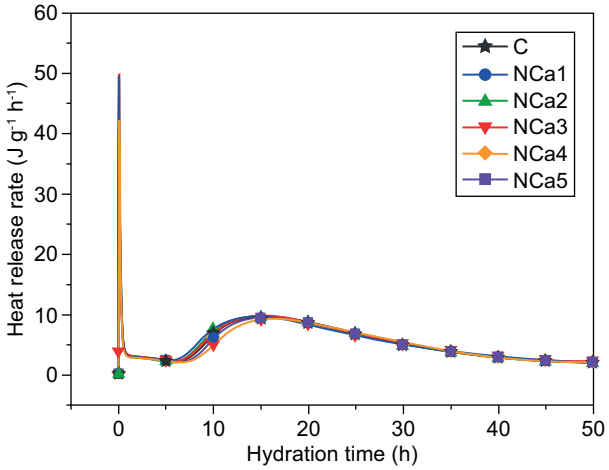

a)

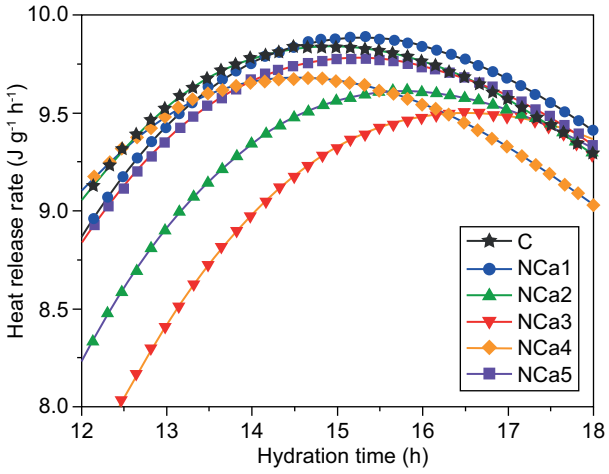

b)

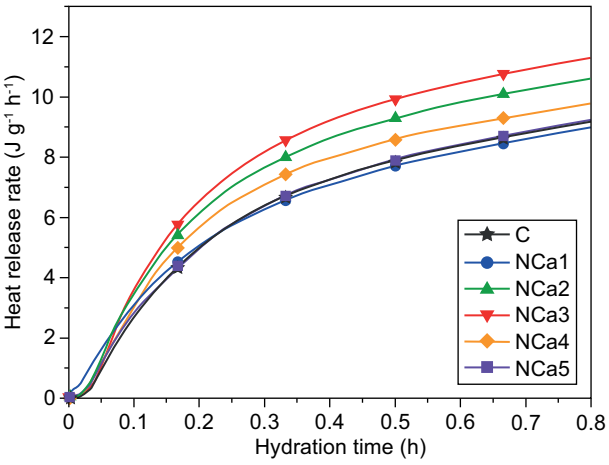

c)

Figure 8. Hydration exothermic curves of the BMSC with the different nano-$CaCO_3$ contents.

CONCLUSIONS

This study described the effect of nano-$CaCO_3$ on the setting and hardening of BMSC. Based on the experimental results, the following general conclusions were obtained.

- The early strength of the BMSC paste can be improved by the addition of nano-$CaCO_3$, and a 3 % nano-$CaCO_3$ content was found to improve the early strength of the BMSC paste by 30.0 %. The effect of the nano-$CaCO_3$ on the strength of BMSC was not obvious in the early stage, and the maximum increase was found to be 15.1 %.
- The phase composition and microstructure of the BMSC cannot be changed by adding nano-$CaCO_3$. The addition of nano-$CaCO_3$ can accelerate the hydration process of the BMSC, and can make the needle-like structure of the 517 phase more compact. Because the amount of massive $Mg(OH)_2$ between the pores is less, the strength is improved.
- The addition of nano-$CaCO_3$ can improve the water resistance of the BMSC by inhibiting the hydration of the BMSC in water to form the crystalline phase of $Mg(OH)_2$, which is disadvantageous to the strength of the cement. Moreover, it can protect the crystals and effectively prevent the massive hydrolysis of the 517 phase. Therefore, the high strength of the BMSC is maintained, and its water resistance is improved.
- The addition of nano-$CaCO_3$ does not affect the setting and hardening time of the cement.

Acknowledgment

This study was supported by the Natural Science Foundation of China (Grant No. 52002202), the applied fundamental research project of Qinghai Province (Grant No. 2019-ZJ-7005), West Light Foundation of The Chinese Academy of Sciences (Grant No.2020) and the S&T Foundation Platform of Qinghai Province (Grant No. 2018-ZJ-T01).

REFERENCES

1. Chengyou W., Hongfa Y., Huifang Z., Jinmei D., Jing W., Yongshan T. (2015): Effects of phosphoric acid and phosphates on magnesium oxysulfate cement. Materials and Structures, 48(4), 907-917. doi: 10.1617/s11527-013-0202-6
2. Deng D. (2003): The mechanism for soluble phosphates to improve the wat er resistance of magnesium oxychloride cement. Cement and Concrete Research, 33(1), 311-317. doi: 10.1016/S0008-8846(03)00043-7
3. Demediuk T., Cole W., Hueber H. (1955): Studies on magnesium and calcium oxychlorides. Australian Journal of Chemistry, 8(2), 215-233. doi: 10.1071/CH9550215
4. Kahle K. (1972): Mechanism formation of magnesium-sulfate cements. Silikatechnik, 23(5), 148-151.
5. Chengyou W. (2014): Fundamental theory and civil engineering application of basic magnesium sulfate cement. Chinese Academy of Sciences.
6. Bruno Fiorio. (2005): Wear characterization and degradation mechanisms of a concrete surface under ice friction. Construction and Building Material, 19(5), 366-375. doi: 10.1016/j.conbuildmat.2004.07.020
7. Chengyou W., Sainan X., Wuyu Z., Ningshan J., Huifang Z., Hongfa Y. (2016): Study on hydration mechanism of basic magnesium sulfate cement. Journal of Functional Materials, 211(47), 120-130. doi: 10.3969/j.issn.1001-9731.2016.11.024

a. Jinmei D., Hongfa Y., Liming Z. (2010): Study on experimental conditions for determination of active MgO content by hydration method. Journal of Salt Lake Research, 18(1), 38-41.

[8. Chunli B. (1996): Development and prospect of nanoscience and Technology. Chinese Science Bulletin, S1, 4-9.

9. Zhongtai Z., Yuanhua L., Zilong T., Junying Z. (2000): Nanometer materials & nanotechology and their application prospect. Journal of Materials Engineering, 3, 42-47. doi: 10.3969/j.issn. 1001-4381.2000.03.012
10. Fangfang W. (2007): Research and application of nanometer materials. Chemical Engineering & Equipment, 3, 38-40. doi: 10.3969/j.issn.1003-0735.2007.03.011
11. Shuangsheng Z., Gentao Z. (1997): Preparation and application of nanometer materials. Chemical World, 38(8), 399-401.
12. Shikao S. (2001): Characteristics and applications of nanometer materials. University Chemistry, 16(2), 39-42. doi: 10.3969/j.issn.1000-8438.2001.02.009
13. Wenxuan Z., Yue Z. (2012): Application of nanometer materials and nanotechnology in building materials. Henan Building Materials, 2, 24-26. doi: 10.3969/j.issn.1008-9772.2012.02.013
14. Liguang X., Jiancheng Z., Zhenhai M. (2003): Nanotechnology and its application in building materials. Journal of Jilin Architectural and Civil Engineering, 20(1), 27-32. doi: 10.3969/j.issn.1009-0185.2003.01.007
15. Runping S. (2010): Application of nano-technology in the field of building materials. Research & Application of Building Materials, 12, 9-11. doi:10.3969/j.issn.1009-9441.2010.12.004
16. Jiayuan Y., Wensheng Z. (2020): Research progress on nano-modified alkali-activated cementitious materials. Journal of The Chinese Ceramic Society, 8, 1263-1277. doi: 10.14062/j.issn.0454-5648.20190521
17. Jianping Z., Aihu F., Xijian W. (2013): Research progress of the application of Nanomaterials in Cement-based Materials. New Chemical Materials, 41(10), 162-164. doi: 10.3969/j.issn.1006-3536.2013.10.054
18. Chong W., Xincheng P., Fang L., Chaojun W., Jianhua W. (2003): Feasibility study on nano particle materials used in cement based materials. New Building Materials, 2, 22-23. doi: 10.3969/j.issn.1001-702X.2003.02.010
19. Roychand R., Saman SD, Setunge S., Law D. (2017): A quantitative study on the effect of nano SiO_2, nano Al_2O_3 and nano $CaCO_3$ on the physicochemical properties of very high volume fly ash cement composite. European Journal of Environmental and Civil Engineering, 24(6), 724-739. doi: 10.1080/19648189.2017.1418681
20. Pan F., Honglei C., Xin L., Shaoxiong Y., Xin S., Qianping R. (2020): The significance of dispersion of nano-SiO_2 on early age hydration of cement pastes. Materials & Design, 186, 108320-108330. doi: 10.1016/j.matdes.2019.108320
21. Nazari A., Riahi S. (2010): The effects of zinc dioxide nanoparticles on flexural strength of self-compacting concrete. Composites Part B: Engineering, 42(2), 167-175. doi: 10.1016/j.compositesb.2010.09.001
22. Kadhim AS., Atiyah AA., Salih SA. (2020): Properties of self-compacting mortar containing nano cement kiln dust. Materials Today: Proceedings, 20, 499-504. doi: 10.1016/j.matpr.2019.09.177
23. Wang C., Zhang C., Liu J. C., Li Z. Y., Yin D. D. (2016): Influence of nano-$CaCO_3$ on hydration characteristic of Portland cement. Bulletin of the Chinese Ceramic Society, 35, 824-830.
24. Tao M., Yue Y., Zhongjia W. (2017): Effect of nano-$CaCO_3$ slurry on the mechanical properties and micro-structure of concrete with and without fly ash. Composites Part B: Engineering, 117, 124-129. doi: 10.1016/j.compositesb.2017.02.030
25. Rui L., Huigang X., Jishuang G., Junjie D., Min L. (2020): Effect of nano-$CaCO_3$ and nano-SiO_2 on improving the properties of carbon fibre-reinforced concrete and their pore-structure models. Construction and Building Materials, 244, 118297. doi: 10.1016/j.conbuildmat.2020.118297